Damage Identification with Model Updating: A Bayesian Approach

Michael L. M. de Souza[1], Ney Roitman[1], Daniel A. Castello[2]

[1]*Civil Engineering Department of Universidade Federal do Rio de Janeiro*
michael.souza@coc.ufrj.br, roitman@coc.ufrj.br
[2]*Mechanical Engineering Department of Universidade Federal do Rio de Janeiro*
castello@mecanica.coppe.ufrj.br

Abstract. Identifying structural damage is complex due to various uncertainties such as boundary conditions, material properties, and damping behaviours. This study uses a Bayesian framework called Approximate Bayesian Computation (ABC) to address the challenge of damage identification. The method can estimate unknown parameters while considering the lack of knowledge about the most suitable damping model for the system. The conventional damage identification problem is reframed as a structural anomaly, with the primary objective being to estimate the position and magnitude of the lumped masses attached to the experimental rig. Ultimately, this framework provides the posterior probability density function (target PDF) of the position and magnitude of the attached mass without relying on prior knowledge of damping behaviour.

Keywords: damage identification, structural health monitoring (SHM), bayesian inference, model updating.

1 Introduction

Usually, dynamic analyses are performed to verify structural damage. It is based on the premise that damaged structures will significantly modify some dynamic characteristics, such as vibration modal shape, natural frequencies, and the frequency response function (FRF) due to variations in the stiffness, mass, or energy dissipation properties regarding the intact structure, R.Farrar and Worden [1]. Beck Beck [2] introduced the Bayesian system identification approach, and Simoen et al. [3] expounded on the necessity of uncertainty quantification in damage identification by applying the Bayesian and Fuzzy approaches in a reinforced concrete beam structure measured in an intact and damaged scenario. Comprehensive damage identification and model updating reviews can be found in R.Farrar and Worden [1], Friswell [4].

The model updating approach was created to increase the accuracy of model predictions by tuning its parameters, Simoen et al. [3], Mottershead and Friswell [5]. For instance, the Bayesian Finite Element (FE) model updating technique is one of the most applied methodologies in parameter estimation and damage identification problems. Based on Bayes' Theorem Kaipio and Somersalo [6], the main goal is to fit the computational prediction with the measured counterpart usually extracted from engineering structures. Nevertheless, some problems exist, such as in the works by [7–9] where building a likelihood function, a crucial input in Bayes' Theorem, is not feasible. In those scenarios, a derivative method called Approximate Bayesian Computation (ABC) can be used because it is unnecessary to formulate a likelihood function, Toni et al. [10]. In the context of dynamical systems, Abdessalem et al. [11] used the ABC method proposed by Toni et al. [10] in a comprehensive toy problem, Vakilzadeh et al. [12] applied the ABC proposed by [13] to infer uncertain parameters and select models on nonlinear dynamic systems, and Castello and Ritto [14] employed an ABC framework for model selection and parameter estimation of drill-string oil & gas problem.

This paper uses the ABC via Sequential Monte Carlo proposed by Toni et al. [10] to evaluate whether the experimental rig is damaged without any previous information. It is achieved by employing model selection so that the most suitable model provides the integrity status of the aluminium beam. The present strategy estimates the position and magnitude of the lumped masses attached to the supported beam, considering only one set of measured data throughout the inference process.

2 Governing equation

The present problem holds a linear formulation of the classical dynamical analysis, ruled by Equation 1, Géradin and Rixen [15].

$$\mathbf{M}\ddot{\mathbf{u}}(t) + \mathbf{D}\dot{\mathbf{u}}(t) + \mathbf{K}\mathbf{u}(t) = \mathbf{F}(t) \tag{1}$$

where $\mathbf{M}$ stands for the mass matrix, $\mathbf{F}$ refers to the external force ascribed to the system, $\mathbf{u}$ contains the displacement vector, and $\dot{\mathbf{u}}$ its first-time derivative. The restoration force can be described as a function of the $\mathbf{K}$, known as the stiffness matrix, and the dissipation force $\mathbf{D}$ known as the damping matrix. One of the adopted models for the damping matrix is according to Equation 2.

$$\mathbf{D} = \alpha\mathbf{M} + \beta\mathbf{K} \tag{2}$$

where α and β are positive-user-defined constants. On the other hand, the damping can be modelled by Equation 3, which holds for constant damping.

$$\mathbf{D} = [\mathbf{\Phi}^{-1}]^T \, 2\,(\zeta^* \, \mathbf{I})\, \mathbf{\Omega}\, [\mathbf{\Phi}^{-1}]^T \tag{3}$$

where $\mathbf{\Phi}$ holds for the eigenvector matrix, in which $(\bullet)^{-1}$ and $(\bullet)^T$, stand for its inverse and transpose respectively. ζ^* represents a constant damping rate adopted, $\mathbf{I}$ the identity matrix and $\mathbf{\Omega}$ the eigenvalue matrix.

3 Bayesian model updating approach

The unknown parameters of a phenomenon of interest can be modelled as random variables in the Bayesian framework, [6]. These variables may be assembled in a vector $\boldsymbol{\theta}$, where $\pi(\boldsymbol{\theta})$ summarizes their probability density function (pdf).

$$\pi(\boldsymbol{\theta}\,|\mathbf{y}) \propto \pi(\mathbf{y}\,|\boldsymbol{\theta})\,\pi(\boldsymbol{\theta}) \tag{4}$$

where $\mathbf{y}$ holds for structure's dynamical data, $\pi(.|.)$ refers to the conditional probability density function and $\pi(.)$ the pdf itself. In this regarding, $\pi(\boldsymbol{\theta}\,|\,\mathbf{y})$ is the posterior distribution, often called *target* distribution, $\pi(\mathbf{y}\,|\boldsymbol{\theta})$ the likelihood function and $\pi(\boldsymbol{\theta})$ the prior.

One sampling method commonly used in an ABC framework is the ABC Sequential Monte Carlo or ABC-SMC. It smoothly evolves a target distribution by drawing sample particles from each intermediate population, i.e. $\pi_{prior}, \cdots \pi_t, \cdots, \pi_{target}$ because of the importance sampling technique, and its generalization, sequential importance sampling *SIS*, both proposed by Del Moral et al. [16, 17]. This ABC method demands a cost function, a comparative metric, to evaluate the closeness of the computed and measured data. In this paper, it is noted as $\rho(\mathbf{y}, \mathbf{y}^m)$, in which $\rho(\mathbf{y}$ and $\mathbf{y}^m)$ are respectively the experimental and computational data respectively. With any error assessment, one should adopt a threshold discrepancy value, which is noted as ϵ.

The comparison metric plays a central role in the inference process. It is the framework feature that drives the accept-reject-sample step and it is frequently an *ad hoc* user-predefined hypothesis or grounded on literature knowledge. In the present investigation, one has proposed the relative difference of natural frequencies, Equation 5 as the comparison metric.

$$\rho = \left| \frac{\boldsymbol{\omega} - \boldsymbol{\omega}^m}{\boldsymbol{\omega}} \right| \tag{5}$$

where $\boldsymbol{\omega}$ stands for the vector of the first six natural frequencies experimentally measured, and $\boldsymbol{\omega}^m$ its computational model counterpart, and $|.|$ refers to the l^2-norm. Table 1 details the adopted models.

Therefore, after accepting a pre-defined number of $\boldsymbol{\theta}^*$ referred to henceforth as *particles*, the ABC algorithm provides an approximation of the target distribution given by Equation 6, where the tolerance value ϵ indicates the similarity level of both probability density functions.

$$\pi(\boldsymbol{\theta}|\rho(\mathbf{y}, \mathbf{y}^m) \leq \epsilon) \approx \pi(\boldsymbol{\theta}|\mathbf{y}) \tag{6}$$

A key aspect of building the prior statistical model is that every random variable had been designed grounded on the premise of being mutually independent and constrained in pdf's domain detailed as follows: $\pi(m) : \{m \in \mathbb{Z}\,|\,m \sim \mathcal{U}(1,7)\}$ (prior of model M1 until M7), $\pi(E) : \{E \in \mathbb{R}\,|\,E \sim \mathcal{U}(7,8)\}[10^{10}$ kPa] of the Young's modulus, $\pi(X) : \{X_m \in \mathbb{R}\,|\,X \sim \mathcal{U}(0,L)\}$ [m] for the lumped mass position, and $\pi(M) : \{M \in \mathbb{R}\,|\,M \sim \mathcal{U}(0,0.5)\}$ [kg] its magnitude. As for the proportional damping coefficient: $\pi(\alpha) : \{\alpha \in \mathbb{R}\,|\,\alpha \sim \mathcal{U}(0,5)\}[10^{-1}s^{-1}]$, and $\pi(\beta) : \{\beta \in \mathbb{R}\,|\,\beta \sim \mathcal{U}(0,15)\}[10^{-6}$ s]. It is important to highlight that $\mathcal{U}$ holds for the uniform probability density function. These values are based on previous investigations of the present experimental setup, [18].

Table 1. Outline of the adopted models.

Id.	Hypothesis		Random vector
	Integrity	Damping	
M1	damaged	undamped	$\boldsymbol{\theta} = \{E\,,\,X\,,\,M\}^T$
M2	damaged	proportional	$\boldsymbol{\theta} = \{E\,,\alpha\,,\beta\,,\,X\,,\,M\}^T$
M3	damaged	$\alpha = 3.1$ and $\beta = 9.0$	$\boldsymbol{\theta} = \{E\,,\,X\,,\,M\}^T$
M4	damaged	constant	$\boldsymbol{\theta} = \{E\,,\,X\,,\,M\}^T$
M5	non-damaged	undamped	$\boldsymbol{\theta} = \{E\}^T$
M6	non-damaged	proportional	$\boldsymbol{\theta} = \{E\,,\,\alpha\,,\,\beta\}^T$
M7	non-damaged	constant	$\boldsymbol{\theta} = \{E\}^T$

4 Experimental rig

The experimental setup, Figure 1, consists of a supported aluminium beam with a 1.464 mm length in a rectangular cross-section shape with 76.2 mm width, 6 mm height, and approximately 2700 kg/m^3 of mass density. The dynamic analysis was performed through consecutive impacts provided by a hammer in a single spot. All measurements were recorded with an acquisition frequency of 1 kHz and filtered by a digital low-pass filter of 250 Hz. Further details of the experimental set-up and model information of acquisition and measurement rigs can be found in Souza et al. [18].

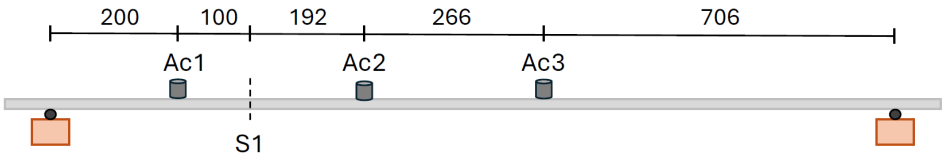

Figure 1. Illustrative scheme of experimental rig.

One rigid block was adopted and attached to the beam length. Its true mass magnitude is 158.4 g, positioned at 0.3 m. It should be stressed that the magnitude of the rigid block represents 9 % of the total beam mass.

Two in-house programs were used to post-process the vibration data Andrade [19], Bucher [20] to assess modal properties and frequency domain response. The experimental data vectors, in each vibration mode, contain the expected values of the natural frequency ω extracted from every performed analysis and can be viewed in Table 2.

Table 2. Natural frequencies extracted from experimental data.

Vibration Mode	ω	σ
1st	6,59	0,01
2nd	25,19	0,01
3rd	57,16	0,03
4th	104,32	0,14
5th	165,25	0,23
6th	234,53	1,53

5 Results and discussion

Figure 2 depicts the posterior pdfs of X and M in the proposed Bayesian framework, considering the relative difference of natural frequencies as the comparison metric. This result indicates that one could access the actual condition of the aluminium beam because M1, M2, M3 and M4 stand for a damaged structure. Interestingly, it is impossible to select the most reliable model at first glance at this level of agreement since all the predictions regarding the position and magnitude of mass are equivalent.

Another positive fact for the inference process is that the real position and mass magnitude values are inside each posterior distribution, despite the bi-modal shape of $\pi(X|\mathbf{y})$. This behaviour, that is, the bi-modal shape positions' posterior density, may be associated with the global property of the natural frequency because the supported beam is symmetric, and the bi-modal shape is equally spaced from the half point of the structure.

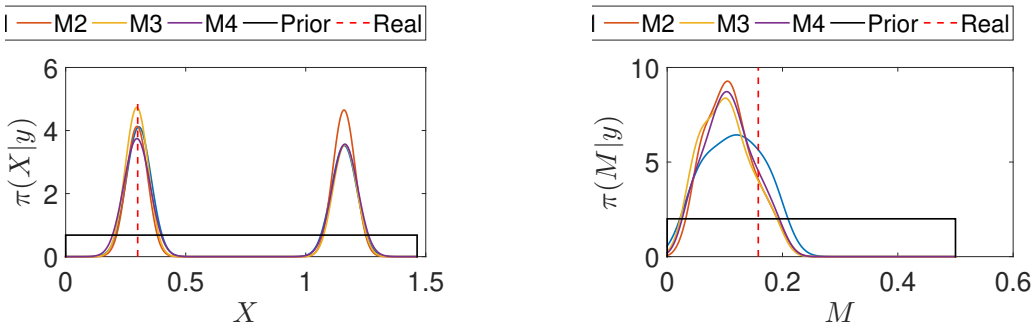

(a) Position. (b) Magnitude

Figure 2. Marginal posterior pdf of the unknown random variables of main interest.

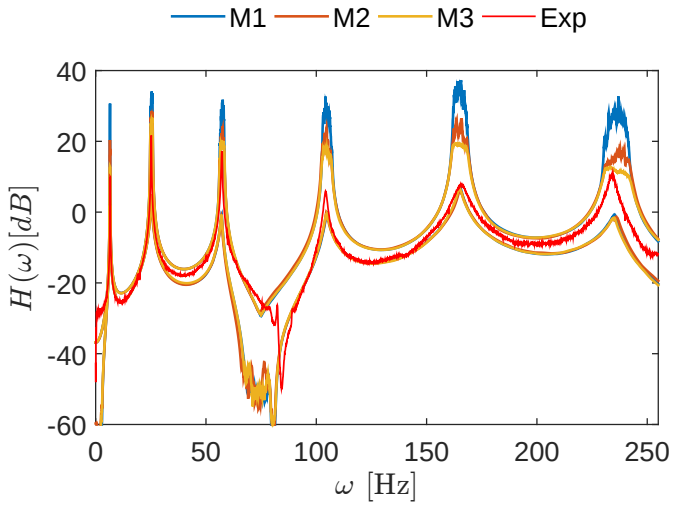

Figure 3. Frequency Response Function (FRF) of models M1, M2, M3, and the aluminium beam at the first sensor (accelerometer) positioned at 0.2 m of beam's span.

Figure 3 details a draft analysis of the uncertainty propagation regarding the Frequency Response Function (FRF) for models M1, M2 and M3. It describes the 90 % credibility interval of computational predictions, which is the 5% and 95% percentiles (the lower and upper boundary curves for each model). The experimental FRF is plotted to guide the analysis. In this context, there is a significant difference between the models, especially regarding the amplitude peak near the natural frequency. This result was already expected due to the fundamental hypotheses of the damping behaviour of each model. M2 and M3 are proportional models, and M1 is undamped, which explains its higher amplitude response.

Figures 4 and 5 show the comparison between the vibration mode peaks for every model regarding the FRF. They closely examine the vicinity of the FRF's peaks (left side figures) and the marginal posterior distribution of each peak (right side figures) for the 1st up to 6th vibration modes. In this context, models M1 and M2 capture

the experimental peak at the 1st, 3rd and 6th which means that the estimated experimental peak is inside of the pdf domains. M1 predictions are significantly higher for all vibration modes since their fundamental hypothesis disregards damping behaviour. The low variability provided by M3 is because α and β parameters of proportional damping have been arbitrarily set beforehand to save computational time, and it varies only due to the stochastic nature of the inference process. Finally, the M2 model adopts α and β as random variables, providing higher posterior distribution variability when compared with M3 predictions.

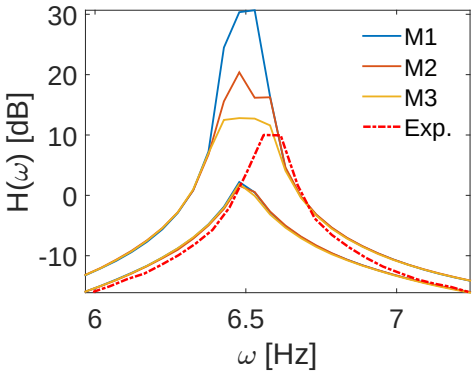

(a) FRF of the 1st vibration mode.

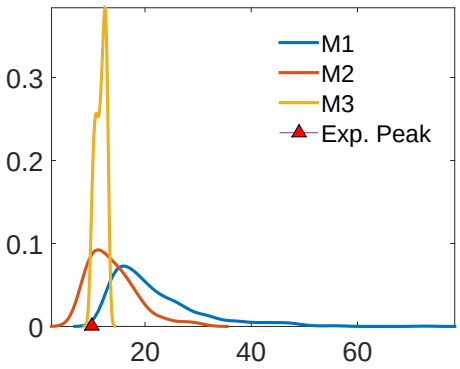

(b) Marginal distributions of the 1st vibration mode peaks. Legend: x-axis holds for $H(\omega)\ [dB]$ and y-axis stands for $\pi(H|\mathbf{y})$.

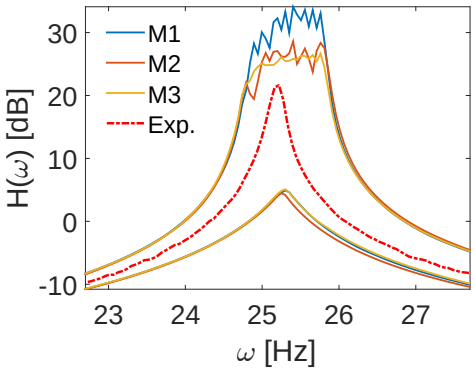

(c) FRF of the 2nd vibration mode.

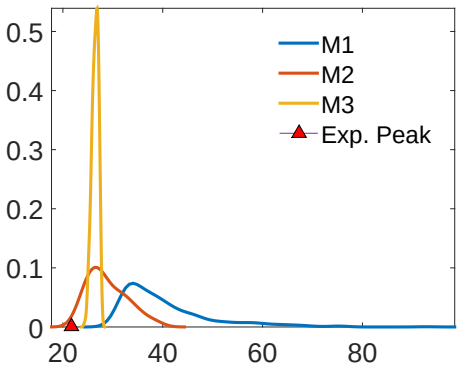

(d) Marginal distributions of the 2rd vibration mode peaks. Legend: x-axis holds for $H(\omega)\ [dB]$ and y-axis stands for $\pi(H|\mathbf{y})$.

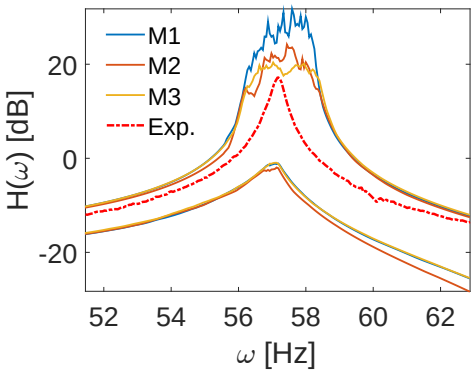

(e) FRF of the 3rd vibration mode.

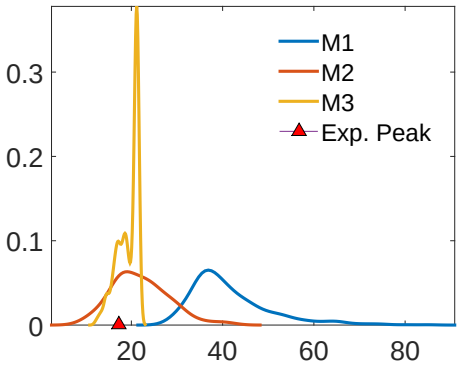

(f) Marginal distributions of the 3rd vibration mode peaks. Legend: x-axis holds for $H(\omega)\ [dB]$ and y-axis stands for $\pi(H|\mathbf{y})$.

Figure 4. Frequency Response Function for the first 3 vibration modes.

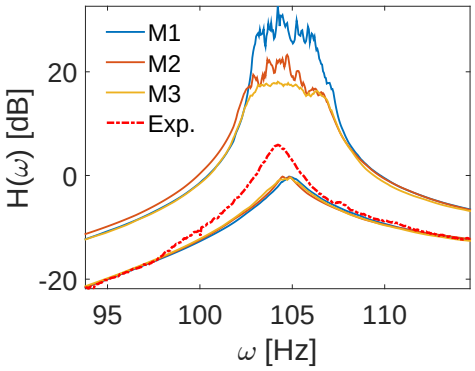

(a) FRF of the 4th vibration mode.

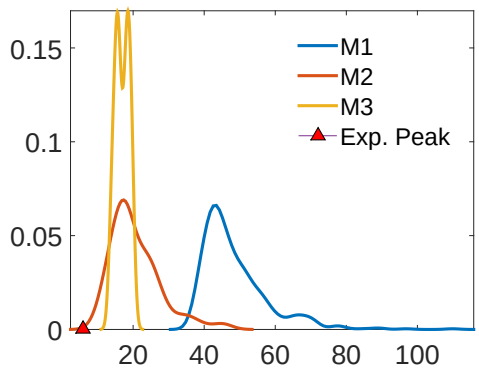

(b) Marginal distributions of the 4rd vibration mode peaks. Legend: x-axis holds for $H(\omega)$ $[dB]$ and y-axis stands for $\pi(H|\mathbf{y})$.

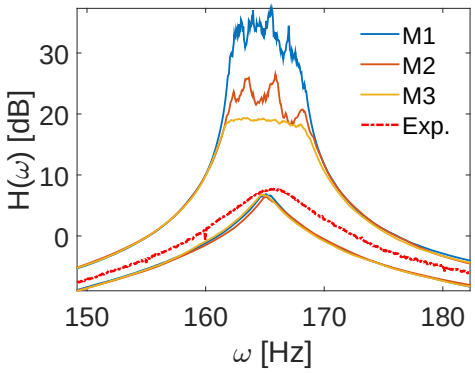

(c) FRF of the 5th vibration mode.

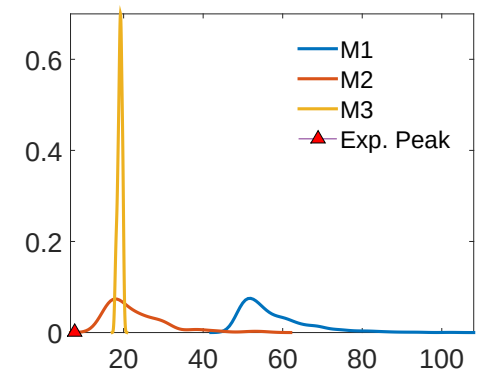

(d) Marginal distributions of the 5rd vibration mode peaks. Legend: x-axis holds for $H(\omega)$ $[dB]$ and y-axis stands for $\pi(H|\mathbf{y})$.

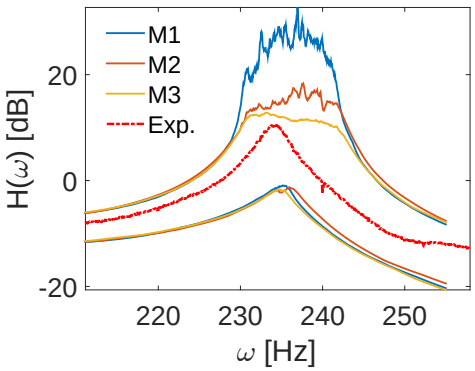

(e) FRF of the 6th vibration mode.

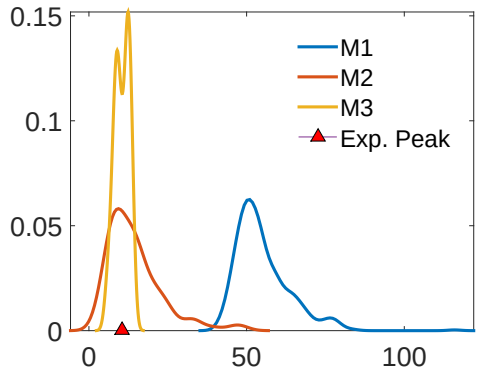

(f) Marginal distributions of the 6rd vibration mode peaks. Legend: x-axis holds for $H(\omega)$ $[dB]$ and y-axis stands for $\pi(H|\mathbf{y})$.

Figure 5. Frequency Response Function for the last 3 vibration modes.

6 Conclusions

The proposed ABC-SMC procedure could assess the aluminium beam's proper condition, employing only one measure dataset. The inference process retrieved the position and magnitude of the lumped mass despite the bi-modal shape of the position's posterior pdf. Nevertheless, it still demands further analysis to enhance its reliability. The ongoing research focuses on using different metrics during the acceptance stage at ABC. In particular, a scalar metric considers natural frequency and damping factors, and a scalar metric considers the modal assurance criteria. In addition, other comparison metrics should be tested to evaluate their performance on the ABC-SMC outcome

regarding SHM problems, such as the maximum assurance criterion (MAC) and the modal curvature.

As for the FRF predictions, the computational model has the experimental data inside the 90 % credibility interval. On the other hand, the forecasts for the resonance peaks still demand enhancement in terms of accuracy.

Acknowledgements. This study was financially supported in part by the Coordenação de Aperfeiçoamento de Pessoal de Nível Superior-Brasil (CAPES) under Finance Code 001.

Authorship statement. The authors hereby confirm that they are the sole liable persons responsible for the authorship of this work, and that all material that has been herein included as part of the present paper is either the property (and authorship) of the authors, or has the permission of the owners to be included here.

References

[1] R.Farrar and K. Worden. An introduction to structural health monitoring. *Philosophical Transactions of The Royal Society A*, vol. 42, pp. 303–315, 2006.

[2] J. L. Beck. Bayesian system identification based on probability logic. *Structural Control and Health Monitoring*, vol. 17, n. 7, pp. 825–847, 2010.

[3] E. Simoen, G. D. Roeck, and G. Lombaert. Dealing with uncertainty in model updating for damage assessment: A review. *Mechanical Systems and Signal Processing*, vol. 56-57, pp. 123 – 149, 2015.

[4] M. I. Friswell. Damage identification using inverse methods. *Philosophical Transactions of The Royal Society A*, vol. 42, pp. 393–410, 2006.

[5] J. E. Mottershead and M. I. Friswell. Model updating in structural dynamics: A survey. *Journal of Sound and Vibration*, vol. 167, pp. 347–375, 1993.

[6] J. P. Kaipio and E. Somersalo. *Statistical and Computational Inverse Problems, Applied Mathematical Sciences*. Springer, New York, USA, 1a edition, 2005.

[7] D. A. Castello and J. P. Kaipio. Modeling errors due to timoshenko approximation in damage identification. *International Journal for Numerical Methods in Engineering*, vol. 120, n. 9, pp. 1148–1162, 2019.

[8] G. L. Silva, D. A. Castello, L. Borges, and J. P. Kaipio. Damage identification in plates under uncertain boundary conditions. *Mechanical Systems and Signal Processing*, vol. 144, pp. 106884, 2020.

[9] G. L. Silva, D. A. Castello, and J. P. Kaipio. Damage identification under uncertain mass density distributions. *Computer Methods in Applied Mechanics and Engineering*, vol. 376, pp. 113672, 2021.

[10] T. Toni, D. Welch, N. Strelkowa, A. Ipsen, and M. P. H. Stumpf. Approximate bayesian computation scheme for parameter inference and model selection in dynamical systems. *Journal of the Royal Society*, vol. 128, pp. 187–202, 2009.

[11] A. B. Abdessalem, N. Dervilis, D. Wagg, and K. Worden. Model selection and parameter estimation in structural dynamics using approximate bayesian computation. *Mechanical Systems and Signal Processing*, vol. 99, pp. 306–325, 2018.

[12] M. K. Vakilzadeh, J. L. Beck, and T. Abrahamsson. Approximate bayesian computation by subset simulation for model selection in dynamical systems. *Procedia Engineering*, vol. 199, pp. 1056 – 1061. X International Conference on Structural Dynamics, EURODYN 2017, 2017.

[13] M. Chiachio, J. L. Beck, J. Chiachio, and G. Rus. Approximate bayesian computation by subset simulation. *SIAM Journal on Scientific Computing*, vol. 36, n. 3, pp. A1339–A1358, 2014.

[14] D. A. Castello and T. G. Ritto. Abc for model selection and parameter estimation of drill-string bit-rock interaction models and stochastic stability. *Journal of Sound and Vibration*, vol. 547, pp. 117537, 2023.

[15] M. Géradin and D. J. Rixen. *Mechanical Vibrations, Theory and Application to Structural Dynamics*. John Wiley & Sons Ltd, Chichester, UK, 3 edition, 2015.

[16] P. Del Moral, A. Doucet, and A. Jasra. Sequential monte carlo samplers. *Journal of the Royal Statistical Society: Series B (Statistical Methodology)*, vol. 68, n. 3, pp. 411–436, 2006.

[17] P. Del Moral, A. Doucet, and A. Jasra. Sequential monte carlo for bayesian computation. *Bayesian statistics*, vol. 8, pp. 1–34, 2011.

[18] M. Souza, D. Castello, N. Roitman, T. Ritto, and others. Impact of damping models in damage identification. *Shock and Vibration*, vol. 2019, 2019.

[19] R. F. M. Andrade. *Desenvolvimento de um Sistema para Determinação Experimental de Funções de Resposta em Frequência para Excitações Simples e Múltiplas*. Tese de D.Sc., COPPE/UFRJ, Rio de Janeiro, RJ, Brasil, 1997.

[20] H. F. Bucher. *Metodologias para a Aplicação de Técnicas Tempo-Frequência em Dinâmica Estrutural e ao Método dos Elementos de Contorno*. Tese de D.Sc., COPPE/UFRJ, Rio de Janeiro, RJ, Brasil, 2001.